4860 J. Med. Chem. 2009, 52, 4860–4868
DOI: 10.1021/jm900448m

Journal of Medicinal Chemistry Article

Flaviviral Protease Inhibitors Identified by Fragment-Based Library Docking into a Structure Generated by Molecular Dynamics

Dariusz Ekonomiuk,[†] Xun-Cheng Su,[‡] Kiyoshi Ozawa,[‡] Christophe Bodenreider,[§] Siew Pheng Lim,[§] Gottfried Otting,[‡] Danzhi Huang,*[,†] and Amedeo Caflisch*[,†]

[†]*Department of Biochemistry, University of Zurich, Winterthurerstrasse 190, CH-8057 Zurich, Switzerland,* [‡]*Research School of Chemistry, The Australian National University, Canberra ACT 0200, Australia, and* [§]*Novartis Institute for Tropical Diseases, Biopolis Road 10, 05-01, Chromos, Singapore*

Received April 7, 2009

Fragment-based docking was used to select a conformation for virtual screening from a molecular dynamics trajectory of the West Nile virus nonstructural 3 protease. This conformation was chosen from an ensemble of 100 molecular dynamics snapshots because it optimally accommodates benzene, the most common ring in known drugs, and two positively charged fragments (methylguanidinium and 2-phenylimidazoline). The latter fragments were used as probes because of the large number of hydrogen bond acceptors in the substrate binding site of the protease. Upon high-throughput docking of a diversity set of 18 694 molecules and pose filtering, only five compounds were chosen for experimental validation, and two of them are active in the low micromolar range in an enzymatic assay and a tryptophan fluorescence quenching assay. Evidence for specific binding to the protease active site is provided by nuclear magnetic resonance spectroscopy. The two inhibitors have different scaffolds (diphenylurea and diphenyl ester) and are promising lead candidates because they have a molecular weight of about 300 Da.

Introduction

West Nile virus (WNV[a]) and the closely related Dengue virus are pathogenic members of the flavivirus family. They are transmitted by mosquito bites. There are neither vaccines nor effective drugs to fight encephalitis and other fatal diseases caused by these flaviviruses, and about 2.5 billion people are potential victims.[1] Yet these diseases have received much less attention than other tropical diseases. The nonstructural 3 protease (NS3pro) has been shown to be responsible for cleavage of the viral polyprotein precursor and to play an important role in the replication of flaviviruses.[2,3] In fact, site directed mutagenesis of the NS3pro cleavage sites in the polyprotein precursor abolishes viral infectivity.[3] Therefore, NS3pro is a very promising target for drug development against flaviviridae infections. Further, it is important to note that three peptidomimetic inhibitors of the related hepatitis C virus protease (about 20% sequence identity with NS3pro) are under late-stage clinical development.[4−6] Several studies on the development of peptidic inhibitors against flaviviral proteases have been published,[7−10] but only few nonpeptidic inhibitors have been reported.[11−14]

The flaviviral NS3pro chain adopts a chymotrypsin-like fold with two six-stranded β-barrels. The binding pocket is small and very shallow with the catalytic triad (His51-Asp75-Ser135) located at the cleft between the two β-barrels.[15] It has been reported that the catalytic activity of NS3pro is significantly increased by the presence of a 47-residue region of the nonstructural cofactor 2B (NS2B).[16] Three X-ray structures of WNV NS2B-NS3pro in complex with inhibitors have been solved: with the substrate-based tetrapeptide benzoyl-norleucine-lysine-arginine-arginine-aldehyde (Bz-Nle-Lys-Arg-Arg-H, PDB code 2fp7),[15] with the tripeptide inhibitor 2-naphthoyl-Lys-Lys-Arg-H (PDB code 3e90),[17] and with bovine pancreatic trypsin inhibitor (BPTI, PDB code 2ijo).[18]

Recently, we have identified a small-molecule inhibitor of WNV NS2B-NS3pro by high-throughput docking into the rigid X-ray structure.[14] Given the intrinsic plasticity of the WNV NS2B-NS3pro structure, we decided to take into account flexibility in a second in silico screening campaign.

Currently most of the programs for docking allow for full flexibility of the ligand, while taking into account the flexibility of the receptor is still an area of active development.[19−22] The algorithms accounting for receptor flexibility can be classified into two categories. The first category includes programs that allow for protein conformational changes upon inhibitor binding. Such an induced fit[23] approach can be achieved by considering some of the receptor's degrees of freedom in the search algorithm. It has been shown that flexibility of a few side chains in the binding site may lead to significant improvement of the docking results.[24−26] However, the results depend on the rotamer library and/or selection of flexible residues.[27] Also, it is very difficult to implement backbone flexibility, and thus, this is very often neglected in flexible docking programs. The second group of programs makes use of multiple conformations of the protein target, such as those originating from different X-ray structures (with and without inhibitors)[28] or NMR ensembles,[26,29] or extracted from molecular dynamics (MD) or Monte Carlo simulations.[30−35] The multiple receptor conformations can be subsequently used as targets for docking studies, and it can be assumed that the different conformations represent

*To whom correspondence should be addressed. For D.H.: phone: (+41 44) 635 55 68 ; fax: (+41 44) 635 68 62; e-mail: dhuang@bioc.uzh.ch. For A.C.: phone: (+41 44) 635 55 21; fax: (+41 44) 635 68 62; e-mail: caflisch@bioc.uzh.ch.

[a]Abbreviations: MD, molecular dynamics; WNV, West Nile virus; NS3pro, nonstructural 3 protease; NS2B, nonstructural cofactor 2B.

 Published on Web 07/02/2009

diversity of the substrates present in the dynamics of the unbound receptor. The rationale behind this approach is based on a conformational selection mechanism.[36−39]

Here, we introduce a procedure for selecting a conformation for high-throughput docking from an ensemble of MD snapshots or from a set of experimental structures of the same protein. The selection is based on the results of docking a small set of representative fragments. These fragments can be chosen by exploiting the available knowledge on the natural ligands and/or previously disclosed inhibitors. If such information is not available, the representative fragments can be selected from statistical analysis of the known drugs[40] or using medicinal chemistry experience. In the present application to WNV NS2B-NS3pro, three rigid fragments are docked in 100 snapshots sampled along an MD simulation started from the X-ray structure. The MD conformation with the most favorable binding energy for the three fragments is selected for library docking. The three fragments are benzene, the most frequent ring in known drugs,[40] and two positively charged fragments: methylguanidinum and 2-phenylimidazoline. The latter two are used because known inhibitors of WNV NS2B-NS3pro have positively charged group(s) interacting with several hydrogen bond acceptors in the nonprime part of the substrate binding. The procedure for the selection of an MD conformation on the basis of the docking of relevant molecular fragments is validated by high-throughput docking of a diversity set of 18 694 molecules. Following docking and filtering of poses, five compounds were tested in vitro. For two of these five compounds low-micromolar inhibitory activity and binding affinity are observed in an enzymatic assay and a tryptophan fluorescence quenching assay, respectively. NMR spectroscopy analysis provides evidence that they bind to the substrate binding site of WNV NS2B-NS3pro.

Methods

Preparation of the WNV NS2B-NS3pro Structure for MD. The coordinates of WNV NS2B-NS3pro in the complex with the tetrapeptide aldehyde inhibitor Bz-Nle-Lys-Arg-Arg-H[15] were downloaded from the PDB database (PDB entry 2fp7). All water molecules and the atoms of the inhibitor were removed. The termini, including the spurious termini at the segment missing in the X-ray structure (residues 28−32 in chain B), were neutralized by the $-COCH_3$ group and the $-NHCH_3$ group at the N-terminus and C-terminus, respectively. Side chains of aspartates and glutamates were negatively charged, those of lysines and arginines were positively charged, and histidines were considered neutral. Internal constraints were relaxed by energy minimization using CHARMM[41,42] and the CHARMm force field[43] with a distance dependent dielectric function.

Conformation Selection by Fragment Docking into Multiple MD Snapshots. An essential element of the present study is the sampling of intrinsic protein flexibility by MD and selection of a representative conformation by fragment docking. For sampling, the protein molecule was immersed in a water sphere and MD simulations were performed using the stochastic boundary potential.[44] Solvent molecules beyond 20 Å from the O_γ atom of the Ser135 side chain were deleted, leaving 160 residues in contact with the water sphere. Protein atoms outside the 20 Å sphere were fixed. Furthermore, to prevent the solvent from leaving the sphere, water molecules beyond 18.5 Å from the center of the sphere were restrained by a quartic potential with a well depth of −0.25 kcal/mol at 19.5 Å followed by a smoothly rising repulsion.[44] Atoms within the 18.5 Å inner region of the 20 Å sphere were not restrained. The simulations were prepared and conducted using version c33b1 of CHARMM[41,42] and the CHARMM22 all-atom force field[43] with the TIP3P model of the water molecules. A dielectric constant of 1 was used in the Coulombic energy term, and the default value of 12 Å was employed for the nonbonding truncation threshold with shifting and switching for the Coulombic and van der Waals energy, respectively.[43] The integration step was 2 fs. Before the production run was started, the minimized structure was heated to 300 K during 0.4 ns. Equilibration at 300 K was also 0.4 ns long, while the production run was 1 ns. The protein was stable during the MD simulation with a backbone root-mean-square deviation (rmsd) smaller than 1.0 Å and small fluctuations in the potential energy (see Supporting Information). During the 1 ns production run 100 snapshots were saved every 5000 steps (i.e., every 10 ps) for evaluating the binding energy of three molecular fragments (benzene, methylguanidinium, and 2-phenylimidazoline) observed in several WNV NS2B-NS3pro inhibitors (Supporting Information). Docking of the three fragments and evaluation of binding energy taking into account electrostatic desolvation energy was performed by SEED.[45,46] A conformation accommodating the three fragments with very favorable SEED energy was selected for high-throughput docking.

The total trajectory of 1.8 ns required about 2.5 days on a low cost desktop. After the high-throughput docking study was finished we begun to study the activation process by performing and analyzing a dozen of explicit water MD simulations of 15−80 ns each.[39] Note that these long MD simulations required several months of computer time and were not yet available at the time of the high-throughput docking.

Preparation of the Library of Compounds for Docking. The molecules for docking were selected from the September 2006 version of the ZINC library, which is a free database of commercially available compounds.[47] About 4.37 million compounds from the ZINC library were first clustered on the basis of molecular similarity calculated by the program DAIM[48] using the leader clustering algorithm and a threshold of the Tanimoto coefficient of 0.996. Cluster representatives with molecular weight smaller than 250 Da or with less than two hydrogen bond donors were discarded. Since the S1−S3 subpockets in the substrate binding site are lined by 19 hydrogen bond acceptors and 5 hydrogen bond donors, compounds with multiple hydrogen bond donors are expected to have higher chances to bind. Only 18 694 compounds remained after clustering and filtering from the initial library of more than four million molecules. Final preparation of the 18 694 compounds for docking included the assignment of CHARMm atom types, force field parameters,[49] partial charges,[50,51] and energy minimization with a distance dependent dielectric function.

High-Throughput Docking and Pose Filtering. The fragment-based docking of the database (of clustered and prefiltered compounds) consists of four consecutive steps: (I) decomposition of each molecule of the library into mainly rigid fragments by the program DAIM,[48] (II) fragment docking with evaluation of electrostatic solvation[52,25] by the program SEED,[45,46] (III) flexible docking of each molecule of the library using the position and orientation of its fragments as anchors by the program FFLD,[53,54] and (IV) final filtering of poses. The first three steps are performed by in-house developed computer programs, which have been described previously.[55] Upon docking and CHARMM minimization with distance dependent dielectric function $\varepsilon(r) = 4r$, the two following filters were applied: (1) ratio of van der Waals interaction energy and molecular weight more favorable than −0.09 kcal/g; (2) at least four intermolecular hydrogen bonds. Moreover, a script implemented in CHARMM was used to weed out poses with unfavorable binding modes. This script identified unfavorable interactions between the small molecule and the protein, e.g., a hydrogen bond donor (acceptor) not involved in a hydrogen bond and within a distance of 3.5 Å from another donor (acceptor), or a polar group buried in a hydrophobic cavity. It is important to note that neither the scoring function of FFLD (step III) nor the CHARMM minimization with distance dependent dielectric is

able to identify such unfavorable interactions. A total of 69 790 poses (14% of the total number of poses) of 7057 compounds (38% of all compounds) passed the filter of unfavorable interactions. A total of 480 poses (of 178 compounds) passed all filters and were visually inspected. No scoring function was used in ranking the compounds.

Computational Requirements. As mentioned above, the MD simulation took about 60 h on a single 3.0 GHz Xeon CPU. The in silico screening of the 18 694 compounds, i.e., docking and binding energy evaluation, took about 45 h on a Beowulf cluster of 100 Opteron 1.8 GHz CPUs.

Enzymatic Assay and Tryptophan Fluorescence Quenching Assay. The enzymatic assay with purified protein in solution was performed as reported previously.[7]

Binding was also measured by a competition assay with a noncovalently bound inhibitor (K_d = 4.6 μM) that quenched tryptophan fluorescence upon binding in the protease active site.[56] Then 3.5 μM protein was titrated by this competitive inhibitor (from 0 to 40 μM) in the absence or presence of 50 μM **1** or **2** in 50 mM Tris, pH 7.5, and 50 mM NaCl. An amount of 90 μL of each dilution was thereafter transferred to a UV-star Greiner 96-well microplate. After 1 h of incubation at room temperature, fluorescence was measured at 25 °C on a Biotek Synergy4 microplate reader with λ_{exe} = 280 nm (bandwidth 10 nm) and λ_{em} = 340 nm (bandwidth 20 nm). Fluorescence intensities were corrected for inner-filter effect. K_d values of compounds **1** and **2** were inferred from their effect on the K_d of the reference compound as described previously.[57]

NMR Spectroscopy. Validation of the compounds binding to the NS2B-NS3pro complex by NMR spectroscopy was performed as described previously.[14,58] Briefly, ^{15}N-HSQC spectra were recorded to assess the impact of the compounds on stabilizing the 3D fold of the protein. The K96A single-point mutant of the NS2B cofactor was employed because it significantly reduced self-cleavage, preventing gradual buildup of sample heterogeneities.[59] Samples were prepared in 90% H_2O/10% D_2O, 20 mM HEPES buffer (pH 7.0), and 2 mM DTT. The complexes with compounds **1**, **2**, and **3** (compound **3** refers to durene-bis-carbamimidothioate[14,58] (Figure S3)) were prepared by titrating 0.2, 0.3, and 0.9 mM protein solutions with a concentrated solution of compound in DMSO-d_6 to final concentrations of 1.3, 0.4, and 3.0 mM, respectively. The INPHARMA (interligand NOE for pharmacophore mapping) strategy was used to verify binding of the compounds to the substrate binding site.[60] The binding affinity of compound **1** to WNV NS2B(K96A)-NS3pro was determined by monitoring the chemical shifts of ^{15}N-HSQC cross-peaks as a function of ligand-to-protein concentration ratio. The ligand-to-protein ratio was varied by titrating a 32 mM solution of **1** into a 0.2 mM solution of ^{15}N/^{13}C-labeled WNV NS2B(K96A)-NS3pro.

Analysis of Compounds Purity. Compounds **1** and **2** were purchased from TimTec and Sigma-Aldrich, respectively. Characterization of the purity and identity was carried out by liquid chromatography−mass spectrometry (LCMS). Analytical LCMS was performed on an Applied Biosystems LC1100 with Applied Biosystems API2000 MS, using a PHENOMENEX, Onyx Monolithic C18 column, 50 mm × 4.6 mm. Gradient was run using solvent A (HPLC grade acetonitrile) and solvent B (0.1% formic acid in water) from 95:5 to 5:95 A/B. Final compound purity was assessed using a Waters Acquity UPLC with an Acquity C18 column, 2.1 mm × 50 mm, 1.8 m at 30 °C, gradient of A (0.1% formic acid in water) and B (HPLC grade acetonitrile) of 95:5 to 5:95 A/B. The LCMS analysis yields a purity of 96.4% and 95% for compounds **1** and **2**, respectively.

Availability of the Software. The software suite of programs for high-throughput docking (DAIM, SEED, FFLD), including input files, test cases and documentation, can be downloaded from http://www.biochem-caflisch.uzh.ch.

Results and Discussion

Conformation Selection by Fragment Docking into Multiple MD Snapshots. To select a conformation of WNV NS2B-NS3pro for in silico screening, three representative fragments were docked using SEED[45,46] into each of the 100 conformations saved during the MD run. Benzene is used as a probe because it is the most frequent fragment in the known drugs[40] and in large databases of available compounds (more than 40% of compounds in the ZINC library have a benzene ring).[48] The methylguanidinium group is present in the inhibitors reported by Ganesh et al.,[11] as well as in several

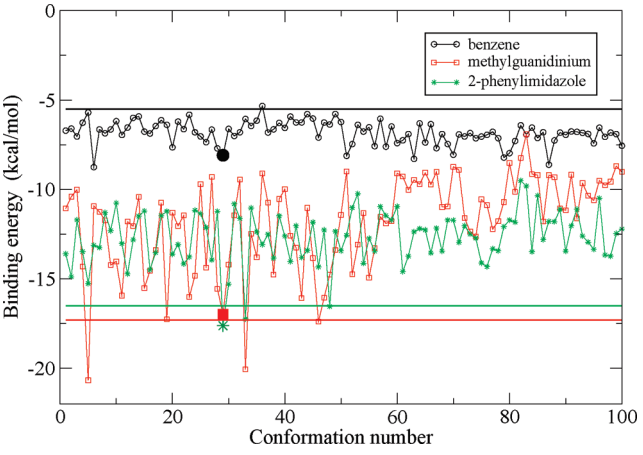

Figure 1. Binding energy of the three fragments docked by SEED[45,46] into 100 conformations saved along the 1 ns MD trajectory of WNV NS2B-NS3pro. The energy values for conformation 29 are emphasized by larger symbols. The horizontal lines represent the binding energy in the X-ray structure (PDB code 2fp7).

Table 1. Calculated Binding Energy (kcal/mol) of the five Best Poses of Each Fragment

fragment	protein conformation[a]	binding energy of best poses[b] 1	2	3	4	5
benzene	X-ray	−5.5	−5.5	−5.4	−5.4	−5.3
	MD	−8.1	−7.1	−6.6	−6.2	−6.1
methylguanidinium	X-ray	−17.3	−16.4	−13.5	−9.7	−9.0
	MD	−17.0	−13.2	−11.3	−10.3	−9.9
2-phenylimidazoline	X-ray	−16.5	−15.2	−13.6	−13.5	−12.0
	MD	−17.6	−16.8	−12.3	−11.9	−11.5

[a] The rows with "X-ray" show the results upon docking into the crystal structure (PDB code 2fp7[15]), while the rows with "MD" contain the results of docking into the conformation 29, i.e., the snapshot saved after 0.29 ns of MD in explicit water. [b] The binding energy is the sum of the van der Waals interaction energy, screened electrostatic interaction, and protein and inhibitor desolvation terms.[45,46] The electrostatic contributions are calculated in the continuum dielectric approximation.[25,52]

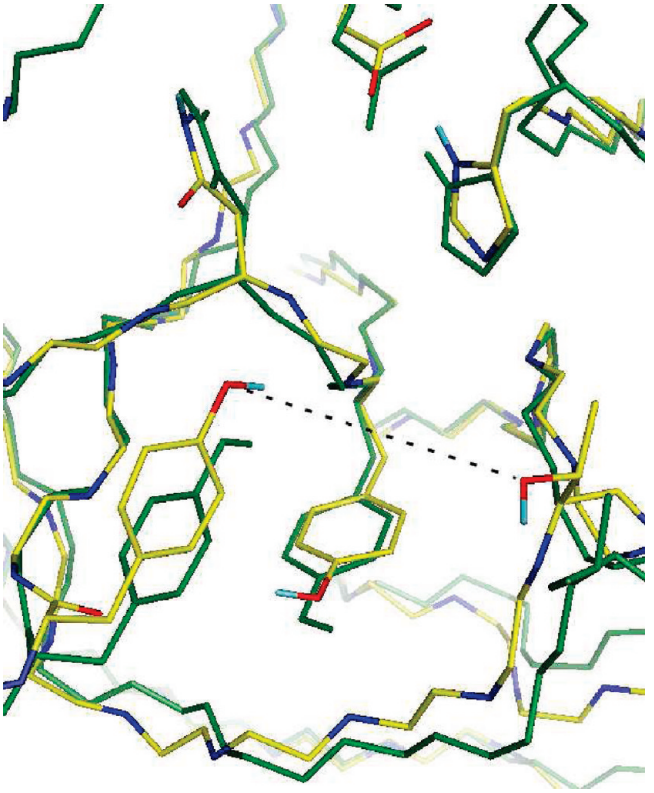

Figure 2. S1 pocket in the X-ray conformation (green) and MD snapshot 29 (colored by atom-type with carbon atoms in yellow) upon optimal overlap of the backbone atoms of WNV NS2B-NS3pro. The rmsd of backbone and side chain atoms of the S1 pocket is 0.3 and 1.3 Å, respectively. Note the decrease of the separation between the side chain hydroxyl oxygens of Tyr161 and Thr132 (black dashed line).

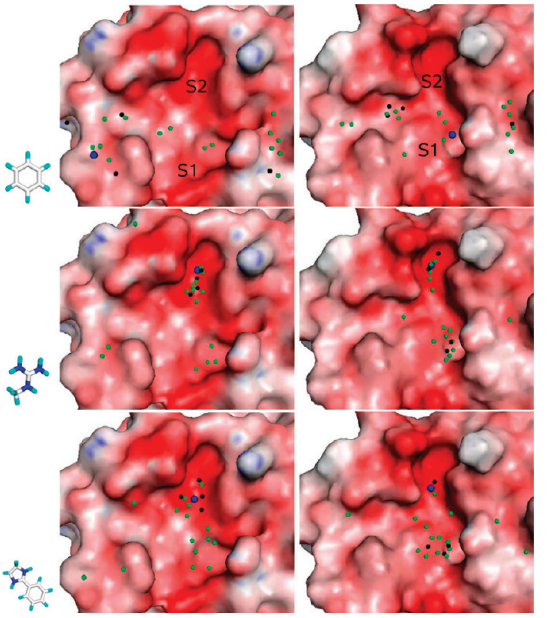

Figure 3. Docking of fragments into the X-ray structure (left) and the MD conformation 29 (right). The geometrical centers of the best 20 poses of benzene (top), methylguanidinium (middle), and 2-phenylimidazoline (bottom) are represented by spheres. The large blue sphere is the best pose among all. This pose together with four black spheres represents the five poses with the most favorable binding energy as evaluated by SEED.[45,46] The surface of WNV NS2B-NS3pro is colored by electrostatic potential with red and blue for negative and positive potential, respectively. The figure was prepared using PyMOL (Delano Scientific, San Carlos, CA), and the APBS program[65] was used for calculation of the electrostatic surface.

tetrapeptidic aldehyde inhibitors with one or more Arg side chains.[7] The 2-phenylimidazoline group is part of low micromolar inhibitors recently described by Bodenreider et al.[56]

The three fragments have very favorable binding energy in the MD conformation 29: −17.0, −17.6, and −8.1 kcal/mol for methylguanidinium, 2-phenylimidazoline, and benzene, respectively (Figure 1 and Table 1). Therefore, conformation 29 is selected for docking. Conformation 33 has more favorable binding energy for methylguanidinium compared with 29 but not for benzene and 2-phenylimidazole. There are a few conformations in the second half of the trajectory (number larger than 50 in Figure 1) with favorable binding energy for benzene, but they do not show optimal binding of the two charged fragments. Note that the binding energy calculated by SEED takes into account electrostatic desolvation, in the continuum dielectric approximation, but does not include the entropy penalty of the protein and ligand upon complex formation so that these binding energy values are more favorable than those measured experimentally for small compounds.

Comparison of X-ray Structure and MD Snapshot Selected by Fragment Docking. The protein structure was stable during MD, and the values of potential, kinetic, and total energy did not change significantly (time series of backbone rmsd and energy are in the Supporting Information). The overlap of the conformation 29 (i.e., the MD snapshot saved after 0.29 ns) with the crystal structure of WNV NS2B-NS3pro shows that the overall topology did not change and the secondary structure is maintained as expected because of the short simulation length (Figure 2). The backbone rmsd between the two structures is 0.8 Å. Some of the side chains in the substrate-binding site show different rotational states in the X-ray structure and MD conformation 29. Also, displacement of the backbone atoms of residues 129−132 results in a reduction by about 2 Å of the Thr132−Tyr161 side chain distance. It is interesting to investigate how the conformational changes in the active site influence the docking and binding energy of the three fragments. The best pose of benzene in the MD conformation 29 (−8.1 kcal/mol, Table 1) forms more favorable van der Waals contacts with atoms in the S1 pocket than the corresponding pose in the X-ray structure, which has a binding energy of −5.1 kcal/mol and ranks only sixth. In fact, the best four poses of benzene in the X-ray structure are located in the S3 and S4 pockets while the fifth is in S1′ (Figure 3).

Both the methylguanidinium and 2-phenylimidazoline have a positive charge and occupy the S1 and S2 pockets in both structures with the most favorable pose in S2. In the X-ray structure both fragments have the five most favorable binding modes in the S2 pocket (Figure 3 and Figure S1 in Supporting Information), while the best five positions are distributed over the S2 and S1 pockets in the MD conformation 29.

High-Throughput Docking. The in silico screening of a diversity set of 18 694 molecules extracted from the ZINC library is schematically represented in Figure 4. The DAIM decomposition of the 18 694 compounds yielded 5883 unique fragments that were used for fragment-based docking by the SEED/FFLD procedure followed by CHARMM minimization in the MD conformation 29 (see Methods). Upon

minimization, only the 480 poses (178 different compounds) that passed a set of energy and structural filters were selected for visual inspection. Poses with poor shape or electrostatic complementarity and/or bad geometry of the intermolecular hydrogen bonds were removed by visual inspection. Finally, five compounds (shown in Supporting Information) were ordered and two of them are active in biochemical and biophysical tests (see below). Interestingly, upon docking and CHARMM minimization into the X-ray structure, the two active compounds did not pass the filters. In the crystal structure, they have a ratio of van der Waals interaction energy and molecular weight of −0.083 kcal/g, which is less favorable than the threshold of −0.090 kcal/g.

Experimental Validation. Compounds **1** and **2** (Figure 4) show low micromolar inhibitory activity for WNV NS2B-NS3pro in the enzymatic assay, as well as micromolar affinity according to NMR chemical shift changes and fluorescence quenching measurements (Table 2). Specific binding to WNV NS2B-NS3pro of these two compounds was validated by NMR spectroscopy using ^{15}N-labeled protein. One-dimensional ^{1}H NMR spectra were used to assess any line broadening experienced by the low-molecular

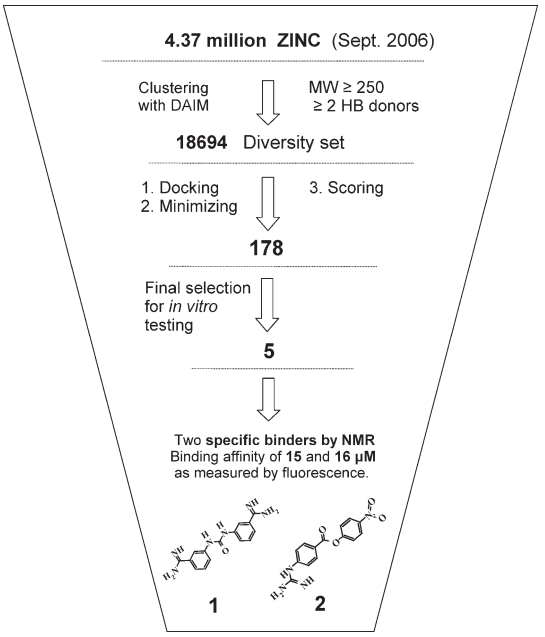

Figure 4. Schematic picture of the in silico screening campaign. The diversity set of 18 694 compounds was derived from the ZINC library by clustering with the program DAIM and filtering out molecules with fewer than two hydrogen bond donors and molecular weight lower than 250 Da. The docking was performed by DAIM/SEED/FFLD[48,45,53] using conformation 29 of WNV NS2B-NS3pro as explained in the text.

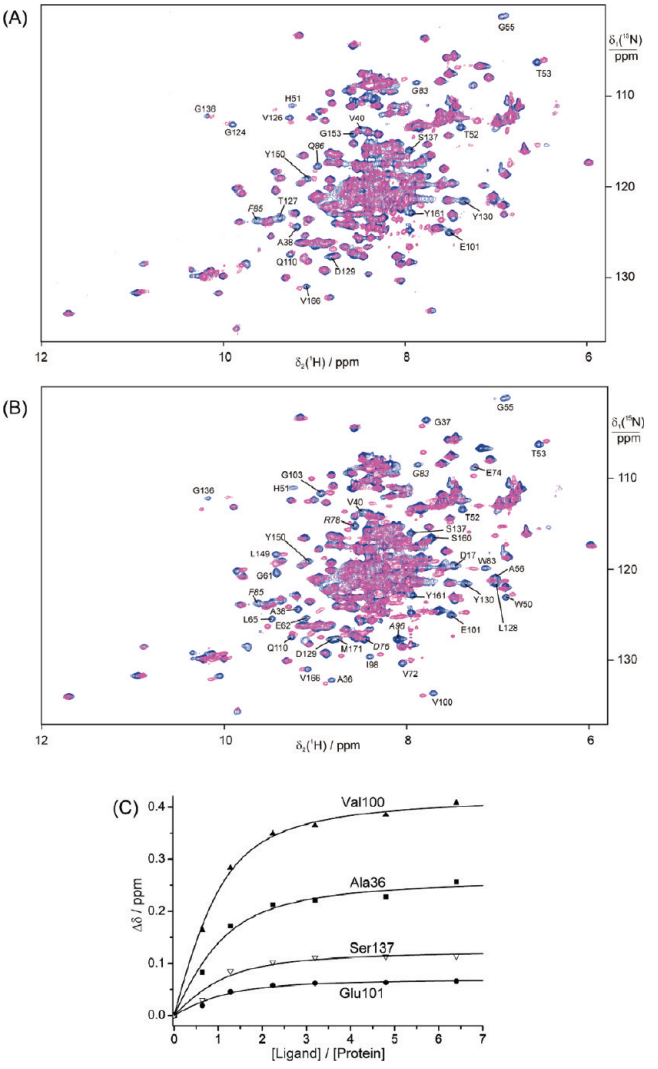

Figure 5. Validation by NMR spectroscopy. All spectra were recorded at 25 °C on a Bruker 800 MHz NMR spectrometer. (A) Superimposition of the ^{15}N-HSQC spectrum of WNV NS2B (K96A)-NS3pro bound to **1** (magenta) onto the corresponding spectrum of the complex with the previously characterized inhibitor durene-bis-carbamimidothioate (compound **3**)[14,58] (blue). Resolved cross-peaks of the complex with **3** are labeled, if the corresponding cross-peak of the complex with **1** is at a significantly different chemical shift. Residues of NS2B are labeled in italics. (B) Same as (A) but with **2** instead of **1**. (C) Binding affinity of **1** to WNV NS2B(K96A)-NS3pro. The plot shows the change in chemical shifts (^{15}N chemical shifts of Ala36, Val100, and Ser137 and ^{1}H chemical shift of the amide proton of Glu101) of WNV NS2B(K96A)-NS3pro as a function of increasing concentration of **1**. The K_d value derived from the curves is about 90 μM (90 ± 20, 90 ± 40, 70 ± 10, and 90 ± 20 μM for the cross-peaks of Ala36, Val100, Glu101, and Ser137, respectively).

Table 2. Experimental Validation of Compounds Identified by Docking into the MD Conformation 29[a]

experiment	measurement	compound 1	compound 2
enzymatic assay[b]	IC_{50}	2.8 ± 0.1 (0.34)	34.2 ± 0.1 (0.28)
tryptophan fluorescence assay[c]	K_d	15 ± 1.6 (0.30)	16 ± 1.8 (0.30)
NMR[d]	K_d	90 ± 40 (0.25)	

[a] The affinity is reported in μM, while the ligand efficiency[64] values (in parentheses) are in kcal/mol per non-hydrogen atom. [b] Concentrations of inhibitors that reduce activity by 50% were measured as described previously.[7] [c] The dissociation constants and error on the fit parameters were measured as described previously.[56] [d] Dissociation constants were measured from changes in chemical shifts as explained in Methods (see also Figure 5C). The K_d value of compound **2** could not be determined by NMR because the exchange between free protein and protein with bound compound was slow on the NMR time scale.

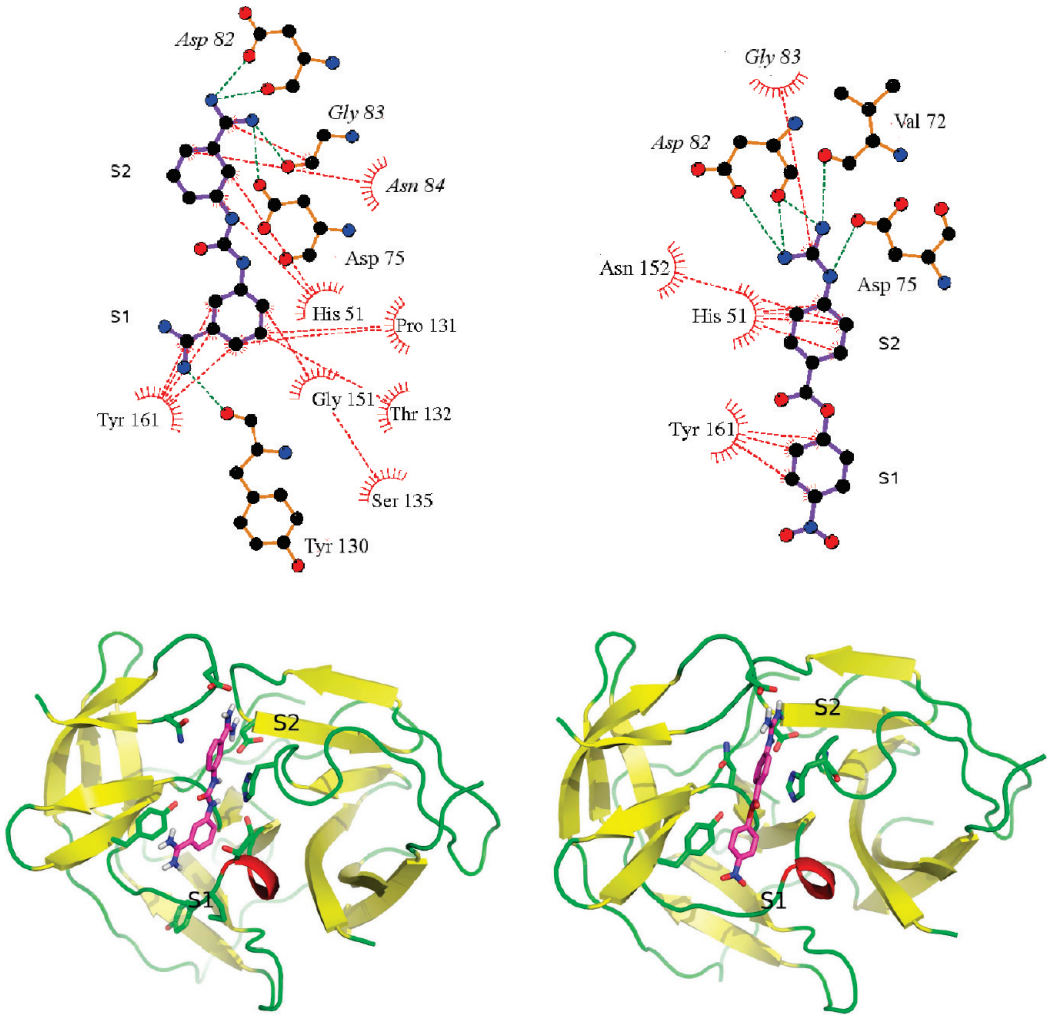

Figure 6. Predicted binding mode of compounds **1** (left) and **2** (right) into WNV NS2B-NS3pro. (Top) The atoms of inhibitors and some of the protease side chains are shown as balls and colored with carbon in black, oxygen in red, and nitrogen in blue. The intermolecular hydrogen bonds are shown by green dashed lines. The intermolecular van der Waals contacts (distance of ≤4 Å) are shown by red dashed lines. Residues of NS2B are labeled in italics. This illustration was prepared by Ligplot.[66] (Bottom) The protease is shown by a cartoon model and colored according to secondary structure. The side chains shown in sticks correspond to those in the top. This illustration was prepared by PyMOL (Delano Scientific, San Carlos, CA).

weight compounds, and ^{15}N-HSQC spectra were recorded to detect responses in the protein. Addition of either **1** or **2** dramatically improved the NMR spectrum of the protease, leading to the appearance of many new cross-peaks (Figure S2 in Supporting Information). In previous studies, similar spectral responses had been reported for compounds that were subsequently confirmed to occupy the substrate binding site by the observation of intermolecular NOEs.[14,58] Binding to the substrate binding site is also suggested by the similarity of the ^{15}N-HSQC spectra of the complexes with compound **1** or **2** with the corresponding spectrum recorded of the previously characterized inhibitor durene-bis-carbamimidothioate (compound **3**; Figure 5A,B). Overall, the chemical shift differences between the different complexes are mostly small, in particular when comparing the complexes with compounds **1** and **3**.

Binding of compound **1** to the substrate binding site of WNV NS2B-NS3pro was ultimately confirmed by a NOESY spectrum recorded in the simultaneous presence of a 12-fold excess of compounds **1** and **3**. The experiment yielded cross-peaks between resonances of the two compounds that were mediated by the protein, indicating magnetization transfer from compound **1** to the protein which is picked up by compound **3** as compound **1** exchanges with compound **3** (Figure S3 in Supporting Information). The corresponding experiment with compound **2** failed because it binds more tightly than compound **3**, leading to transferred NOEs only between resonances of compound **2** (data not shown). Binding of compound **2** in the substrate binding site is indicated by the fact that the amide of the active site histidine (His51) showed some of the largest chemical shift differences between the complexes with different inhibitors (Figure 5). Furthermore, compound **2** dramatically improved the NMR spectrum of the protease as previously observed for inhibitors that occupy the substrate binding site[14,58] (Figure S2B).

The binding affinity of compound **1** was determined by measuring the change of chemical shifts of the amide cross-peaks of Ala36, Val100, Gln101, and Ser137 as a function of increasing concentration of compound **1**. A K_d value of about 90 μM was obtained by fitting (Figure 5C). The residues used for monitoring the binding affinity are located about 10 Å from the substrate binding site. Cross-peaks of residues closer to the active site were either not resolved or suffered from extreme line broadening in the absence of

inhibitor. The binding affinity of compound **2** could not be determined in this way because the exchange between free protein and protein with bound compound was slow on the NMR time scale.

The binding affinity of compound **1** measured by three different experimental techniques ranges from 3 to 90 μM (Table 2). These discrepancies may reflect intrinsic differences in the mechanism of the three assays. The ^{15}N-HSQC NMR spectra report directly on the binding of the compound to the protein, and the binding affinity is derived from the change of ^{15}N and ^{1}H chemical shifts of the backbone amide resonances. On the other hand, the enzymatic assay and tryptophan fluorescence quenching assay are both competitive tests. The IC_{50} is derived in the enzymatic assay by monitoring the competitive binding of **1** and the (nonnatural) substrate (Bz-nKRR-7-amino-4-methylcoumarin), while the K_d in the tryptophan fluorescence assay is obtained by competition with a noncovalently binding inhibitor. Discrepancies are also expected due to different conditions of buffer and pH (for example, the conditions of the IC_{50} measurements include 20% glycerol in the buffer).

Binding Mode. As mentioned above, the binding modes of compounds **1** and **2** were obtained by automatic docking with FFLD[53,54] in the MD conformation 29 followed by CHARMM minimization with rigid protein (Figure 6). The docked structures show binding to the substrate binding site, in agreement with the available NMR data. The 1,3-diphenylurea scaffold of compound **1** links two amidino groups that are involved in hydrogen bonds with acceptor groups in the S1 and S2 pockets. The hydrogen bond acceptor group in S1 is the Tyr130 backbone carbonyl oxygen, and in S2 there are interactions with the Asp75 side chain as well as with the NS2B Asp82 and the Gly83 backbone carbonyl oxygen. The pose of compound **1** is further stabilized by van der Waals interactions between the phenyl ring in the S1 pocket and the side chains of Pro131, Thr132, and Tyr161, as well as between the phenyl ring in the S2 pocket and the side chains of His51 and NS2B Asn84.

The guanidinium group of compound **2** is involved in hydrogen bond interactions with the backbone carbonyl oxygens of Val72 and NS2B Asp82, as well as with the carboxylates of Asp75 and NS2B Asp82. The pose is further stabilized by van der Waals contacts between the phenyl ring in the S2 pocket and the side chains of His51 and Asn152. Moreover, there are van der Waals interactions between the nitrophenyl moiety of compound **2** and the Tyr161 side chain.

Conclusions

We have presented a procedure for selecting from an ensemble of protein conformers a single structure for high-throughput docking of large libraries of compounds. Upon docking of a small set of representative molecular fragments into all conformers, the structure that optimally accommodates these fragments is chosen for high-throughput docking. The fragment-based selection procedure has been applied to an ensemble of 100 snapshots sampled by a MD simulation of WNV NS2B-NS3pro in explicit solvent using benzene, methylguanidinium, and 2-phenylimidazoline as representative fragments. Benzene is the most common ring in known drugs and chemical libraries, while the positive charge of methylguanidinium and 2-phenylimidazoline was expected to favorably interact with the large set of hydrogen bond acceptors in the nonprime part of the substrate binding site of WNV NS2B-NS3pro. Moreover, positively charged functional groups are present in known inhibitors of flaviviral NS3 proteases. It is important to note that our procedure for choosing or prioritizing conformations of the target protein for docking is not restricted to conformations generated by MD but can be applied also to multiple NMR conformers and/or X-ray structures. Furthermore, the representative fragments used for the selection procedure can exploit previous structural knowledge (e.g., kinase-privileged fragments[61]) and/or medicinal chemistry experience (e.g., molecules with druglike moieties[62]).

A diversity set of 18 694 molecules has been docked into the MD snapshot of WNV NS2B-NS3pro selected by the fragment-based procedure. Upon testing of only five compounds, the diphenylurea **1** and diphenyl ester **2** have emerged as low-micromolar inhibitors according to an enzymatic assay and a fluorescence quenching assay. Specific binding of these two inhibitors to the substrate binding site is suggested by the striking similarity of the NMR spectra of WNV NS2B-NS3pro with spectra previously recorded with inhibitors that have been shown to bind to the S1 and S2 pockets.[14,58] The two inhibitors are involved in multiple hydrogen bonds and van der Waals contacts with residues in the S1 and S2 pockets. It is interesting to note that compounds **1** and **2** would not have been identified by docking into the X-ray structure, as their poses do not pass the van der Waals energy filter used in this study. It is likely that the two phenyl rings of compounds **1** and **2** do not fit well in the X-ray structure, as suggested by the calculated binding energy of benzene which is less favorable in the crystal structure than in the MD snapshot selected for docking (Table 1).

Finally, it is possible to combine our procedure for fragment-based selection of a protein conformation from an MD ensemble with a recently reported approach for focusing a chemical library by docking and prioritizing molecular fragments according to their binding energy.[63] The combination of the two methods is expected to efficiently find small molecules that bind to (meta)stable conformers of the target protein presenting orientations of side chains and aperture of active site pockets different from those in the experimentally determined structure.

Acknowledgment. We thank A. Widmer (Novartis Pharma, Basel, Switzerland) for the excellent support with the molecular modeling program WITNOTP which was used for preparing the structures and visual analysis of the results. The calculations were performed on the Matterhorn Beowulf cluster at the Informatikdienste of the University of Zurich.

Supporting Information Available: Structures of known inhibitors, SEED results for methylguanidinium, structures of five compounds suggested for experimental verification, NMR spectroscopy results, and time series of backbone rmsd and energy. This material is available free of charge via the Internet at http://pubs.acs.org.

References

(1) Division of Vector-Borne Infectious Disease. West Nile virus homepage. Centers for Disease Control and Prevention. http://www.cdc.gov/ncidod/dvbid/westnile (2007).
(2) Mukhopadhyay, S.; Kuhn, R. J.; Rossmann, M. G. A structural perspective of the flavivirus life cycle. *Nat. Rev. Microbiol.* **2005**, *3*, 13–22.

(3) Chappell, K. J.; Stoermer, M. J.; Fairlie, D. P.; Young, P. R. Insights to substrate binding and processing by West Nile virus NS3 protease through combined modeling, protease mutagenesis, and kinetic studies. *J. Biol. Chem.* **2006**, *281*, 38448–38458.
(4) Perni, R. B.; Almquist, S. J.; Byrn, R. A.; Chandorkar, G.; Chaturvedi, P. R.; Courtney, L. F.; Decker, C. J.; Dinehart, K.; Gates, C. A.; Harbeson, S. L.; Heiser, A.; Kalkeri, G.; Kolaczkowski, E.; Lin, K.; Luong, Y.-P.; Rao, B. G.; Taylor, W. P.; Thomson, J. A.; Tung, R. D.; Wei, Y.; Kwong, A. D.; Lin, C. Preclinical profile of VX-950, a potent, selective, and orally bioavailable inhibitor of hepatitis C virus NS3-4A serine protease. *Antimicrob. Agents Chemother.* **2006**, *50*, 899–909.
(5) Malcolm, B. A.; Liu, R.; Lahser, F.; Agrawal, S.; Belanger, B.; Butkiewicz, N.; Chase, R.; Gheyas, F.; Hart, A.; Hesk, D.; Ingravallo, P.; Jiang, C.; Kong, R.; Lu, J.; Pichardo, J.; Prongay, A.; Skelton, A.; Tong, X.; Venkatraman, S.; Xia, E.; Girijavallabhan, V.; Njoroge, F. G. SCH 503034, a mechanism-based inhibitor of hepatitis C virus NS3 protease, suppresses polyprotein maturation and enhances the antiviral activity of alpha interferon in replicon cells. *Antimicrob. Agents Chemother.* **2006**, *50*, 1013–1020.
(6) Seiwert, S. D.; Andrews, S. W.; Jiang, Y.; Serebryany, V.; Tan, H.; Kossen, K.; Rajagopalan, P. T. R.; Misialek, S.; Stevens, S. K.; Stoycheva, A.; Hong, J.; Lim, S. R.; Qin, X.; Rieger, R.; Condroski, K. R.; Zhang, H.; Do, M. G.; Lemieux, C.; Hingorani, G. P.; Hartley, D. P.; Josey, J. A.; Pan, L.; Beigelman, L.; Blatt, L. M. Preclinical characteristics of the hepatitis C virus NS3/4A protease inhibitor itmn-191 (r7227). *Antimicrob. Agents Chemother.* **2008**, *52*, 4432–4441.
(7) Knox, J. E.; Ma, N. L.; Yin, Z.; Patel, S. J.; Wang, W.-L.; Chan, W.-L.; Rao, K. R. R.; Wang, G.; Ngew, X.; Patel, V.; Beer, D.; Lim, S. P.; Vasudevan, S. G.; Keller, T. H. Peptide inhibitors of West Nile NS3 protease: SAR study of tetrapeptide aldehyde inhibitors. *J. Med. Chem.* **2006**, *49*, 6585–6590.
(8) Shiryaev, S. A.; Ratnikov, B. I.; Chekanov, A. V.; Sikora, S.; Rozanov, D. V.; Godzik, A.; Wang, J.; Smith, J. W.; Huang, Z.; Lindberg, I.; Samuel, M. A.; Diamond, M. S.; Strongin, A. Y. Cleavage targets and the D-arginine-based inhibitors of the West Nile virus ns3 processing proteinase. *Biochem. J.* **2006**, *393*, 503–511.
(9) Tomlinson, S. M.; Watowich, S. J. Substrate inhibition kinetic model for West Nile virus NS2B-NS3 protease. *Biochemistry* **2008**, *47*, 11763–11770.
(10) Stoermer, M. J.; Chappell, K. J.; Liebscher, S.; Jensen, C. M.; Gan, C. H.; Gupta, P. K.; Xu, W.-J.; Young, P. R.; Fairlie, D. P. Potent cationic inhibitors of West Nile virus NS2B/NS3 protease with serum stability, cell permeability and antiviral activity. *J. Med. Chem.* **2008**, *51*, 5714–5721.
(11) Ganesh, V. K.; Muller, N.; Judge, K.; Luan, C.-H.; Padmanabhan, R.; Murthy, K. H. M. Identification and characterization of nonsubstrate based inhibitors of the essential dengue and West Nile virus proteases. *Bioorg. Med. Chem.* **2005**, *13*, 257–264.
(12) Johnston, P. A.; Phillips, J.; Shun, T. Y.; Shinde, S.; Lazo, J. S.; Huryn, D. M.; Myers, M. C.; Ratnikov, B. I.; Smith, J. W.; Su, Y.; Dahl, R.; Cosford, N. D. P.; Shiryaev, S. A.; Strongin, A. Y. HTS identifies novel and specific uncompetitive inhibitors of the two-component NS2B-NS3 proteinase of West Nile virus. *Assay Drug Dev. Technol.* **2007**, *5*, 737–750.
(13) Mueller, N. H.; Pattabiraman, N.; Ansarah-Sobrinho, C.; Viswanathan, P.; Pierson, T. C.; Padmanabhan, R. Identification and biochemical characterization of small-molecule inhibitors of West Nile virus serine protease by a high-throughput screen. *Antimicrob. Agents Chemother.* **2008**, *52*, 3385–3393.
(14) Ekonomiuk, D.; Su, X.-C.; Ozawa, K.; Bodenreider, C.; Lim, S. P.; Yin, Z.; Keller, T. H.; Beer, D.; Patel, V.; Otting, G.; Caflisch, A.; Huang, D. Discovery of a non-peptidic inhibitor of West Nile virus NS3 protease by high-throughput docking. *PloS Neglected Trop. Dis.* **2009**, *3*, e356.
(15) Erbel, P.; Schiering, N.; D'Arcy, A.; Renatus, M.; Kroemer, M.; Lim, S. P.; Yin, Z.; Keller, T. H.; Vasudevan, S. G.; Hommel, U. Structural basis for the activation of flaviviral NS3 proteases from dengue and West Nile virus. *Nat. Struct. Mol. Biol.* **2006**, *13*, 372–373.
(16) Yusof, R.; Clum, S.; Wetzel, M.; Murthy, H. M.; Padmanabhan, R. Purified NS2B/NS3 serine protease of dengue virus type 2 exhibits cofactor NS2B dependence for cleavage of substrates with dibasic amino acids in vitro. *J. Biol. Chem.* **2000**, *275*, 9963–9969.
(17) Robin, G.; Chappell, K.; Stoermer, M. J.; Hu, S.-H.; Young, P. R.; Fairlie, D. P.; Martin, J. L. Structure of West Nile virus NS3 protease: ligand stabilization of the catalytic conformation. *J. Mol. Biol.* **2009**, *385*, 1568–1577.
(18) Aleshin, A. E.; Shiryaev, S. A.; Strongin, A. Y.; Liddington, R. C. Structural evidence for regulation and specificity of flaviviral proteases and evolution of the flaviviridae fold. *Protein Sci.* **2007**, *16*, 795–806.
(19) Carlson, H. A. Protein flexibility and drug design: how to hit a moving target. *Curr. Opin. Chem. Biol.* **2002**, *6*, 447–452.
(20) Teague, S. J. Implications of protein flexibility for drug discovery. *Nat. Rev. Drug Discovery* **2003**, *2*, 527–541.
(21) Teodoro, M. L.; Kavraki, L. E. Conformational flexibility models for the receptor in structure based drug design. *Curr. Pharm. Des.* **2003**, *9*, 1635–1648.
(22) Totrov, M.; Abagyan, R. Flexible ligand docking to multiple receptor conformations: a practical alternative. *Curr. Opin. Struct. Biol.* **2008**, *18*, 178–184.
(23) Koshland, D. E. Application of a theory of enzyme specificity to protein synthesis. *Proc. Natl. Acad. Sci. U.S.A.* **1958**, *44*, 98–104.
(24) Leach, A. R. Ligand docking to proteins with discrete side-chain flexibility. *J. Mol. Biol.* **1994**, *235*, 345–356.
(25) Caflisch, A.; Fischer, S.; Karplus, M. Docking by Monte Carlo minimization with a solvation correction: application to an FKBP−substrate complex. *J. Comput. Chem.* **1997**, *18*, 723–743.
(26) Kaellblad, P.; Todorov, N. P.; Willems, H. M. G.; Alberts, I. L. Receptor flexibility in the in silico screening of reagents in the S1′ pocket of human collagenase. *J. Med. Chem.* **2004**, *47*, 2761–2767.
(27) Alberts, I. L.; Todorov, N. P.; Dean, P. M. Receptor flexibility in de novo ligand design and docking. *J. Med. Chem.* **2005**, *48*, 6585–6596.
(28) Barril, X.; Morley, S. D. Unveiling the full potential of flexible receptor docking using multiple crystallographic structures. *J. Med. Chem.* **2005**, *48*, 4432–4443.
(29) Damm, K. L.; Carlson, H. A. Exploring experimental sources of multiple protein conformations in structure-based drug design. *J. Am. Chem. Soc.* **2007**, *129*, 8225–8235.
(30) Carlson, H. A.; Masukawa, K. M.; McCammon, J. A. Method for including the dynamic fluctuations of a protein in computer-aided drug design. *J. Phys. Chem. A* **1999**, *103*, 10213–10219.
(31) Lin, J.-H.; Perryman, A. L.; Schames, J. R.; McCammon, J. A. Computational drug design accommodating receptor flexibility: the relaxed complex scheme. *J. Am. Chem. Soc.* **2002**, *124*, 5632–5633.
(32) Lin, J.-H.; Perryman, A. L.; Schames, J. R.; McCammon, J. A. The relaxed complex method: accommodating receptor flexibility for drug design with an improved scoring scheme. *Biopolymers* **2003**, *68*, 47–62.
(33) Meagher, K. L.; Carlson, H. A. Incorporating protein flexibility in structure-based drug discovery: using HIV-1 protease as a test case. *J. Am. Chem. Soc.* **2004**, *126*, 13276–13281.
(34) Bisson, W. H.; Cheltsov, A. V.; Bruey-Sedano, N.; Lin, B.; Chen, J.; Goldberger, N.; May, L. T.; Christopoulos, A.; Dalton, J. T.; Sexton, P. M.; Zhang, X.-K.; Abagyan, R. Discovery of antiandrogen activity of nonsteroidal scaffolds of marketed drugs. *Proc. Natl. Acad. Sci. U.S.A.* **2007**, *104*, 11927–11932.
(35) Amaro, R. E.; Baron, R.; McCammon, J. A. An improved relaxed complex scheme for receptor flexibility in computer-aided drug design. *J. Comput.-Aided Mol. Des.* **2008**, *22*, 693–705.
(36) Henzler-Wildman, K. A.; Thai, V.; Lei, M.; Ott, M.; Wolf-Watz, M.; Fenn, T.; Pozharski, E.; Wilson, M. A.; Petsko, G. A.; Karplus, M.; Hbner, C. G.; Kern, D. Intrinsic motions along an enzymatic reaction trajectory. *Nature* **2007**, 838–844.
(37) Lange, O. F.; Lakomek, N.-A.; Fars, C.; Schrder, G. F.; Walter, K. F. A.; Becker, S.; Meiler, J.; Grubmller, H.; Griesinger, C.; de Groot, B. L. Recognition dynamics up to microseconds revealed from an rdc-derived ubiquitin ensemble in solution. *Science* **2008**, *320*, 1471–1475.
(38) Wong, S.; Jacobson, M. P. Conformational selection in silico: loop latching motions and ligand binding in enzymes. *Proteins* **2008**, *71*, 153–164.
(39) Ekonomiuk, D.; Caflisch, A. Activation of the West Nile virus NS3 protease: molecular dynamics evidence for a conformational selection mechanism. *Protein Sci.* **2009**, *18*, 1003–1011.
(40) Bemis, G.; Murcko, M. A. The properties of known drugs. 1. Molecular frameworks. *J. Med. Chem.* **1996**, *39*, 2887–2893.
(41) Brooks, B. R.; Bruccoleri, R. E.; Olafson, B. D.; States, D. J.; Swaminathan, S.; Karplus, M. CHARMM: a program for macromolecular energy, minimization, and dynamics calculations. *J. Comput. Chem.* **1983**, *4*, 187–217.
(42) Brooks, B. R.; Brooks III, C. L.; Mackerell, A. D., Jr.; Nilsson, L.; Petrella, R. J.; Roux, B.; Won, Y.; Archontis, G.; Bartels, C.; Boresch, S.; Caflisch, A.; Caves, L.; Cui, Q.; Dinner, A. R.; Feig, M.; Fischer, S.; Gao, J.; Hodoscek, M.; Im, W.; Kuczera, K.; Lazaridis, T.; Ma, J.; Ovchinnikov, V.; Paci, E.; Pastor, R. W.; Post, C. B.; Pu, J. Z.; Schaefer, M.; Tidor, B.; Venable, R. M.; Woodcock, H. L.; Wu, X.; Yang, W.; York, D. M.; Karplus, M. CHARMM: the biomolecular simulation program.. *J. Comput. Chem.* **2009**, *30*, 1545–1614.

(43) MacKerell, A. Jr.; Bashford, D.; Bellott, M.; Dunbrack, R. Jr.; Field, M.; Fischer, S.; Gao, J.; Guo, H.; Ha, S.; Joseph, D.; Kuchnir, L.; Kuczera, K.; Lau, F.; Mattos, C.; Michnick, S.; Ngo, T.; Nguyen, D.; Prodhom, B.; Roux, B.; Schlenkrich, M.; Smith, J.; Stote, R.; Straub, J.; Wiorkiewicz-Kuczera, J.; Karplus, M. All-atom empirical potential for molecular modeling and dynamics studies of proteins. *J. Phys. Chem. B* **1998**, *102*, 3586–3616.
(44) Brooks, C. L.III; Karplus, M. Deformable stochastic boundaries in molecular dynamics. *J. Chem. Phys.* **1983**, *79*, 6312–6325.
(45) Majeux, N.; Scarsi, M.; Apostolakis, J.; Ehrhardt, C.; Caflisch, A. Exhaustive docking of molecular fragments on protein binding sites with electrostatic solvation. *Proteins: Struct., Funct., Bioinf.* **1999**, *37*, 88–105.
(46) Majeux, N.; Scarsi, M.; Caflisch, A. Efficient electrostatic solvation model for protein-fragment docking. *Proteins: Struct., Funct., Bioinf.* **2001**, *42*, 256–268.
(47) Irwin, J. J.; Shoichet, B. K. ZINC-a free database of commercially available compounds for virtual screening. *J. Chem. Inf. Model* **2005**, *45*, 177–182.
(48) Kolb, P.; Caflisch, A. Automatic and efficient decomposition of two-dimensional structures of small molecules for fragment-based high-throughput docking. *J. Med. Chem.* **2006**, *49*, 7384–7392.
(49) Momany, F.; Rone, R. Validation of the general purpose QUANTA 3.2/CHARMm force field. *J. Comput. Chem.* **1992**, *13*, 888–900.
(50) No, K.; Grant, J.; Scheraga, H. Determination of net atomic charges using a modified partial equalization of orbital electronegativity method. 1. Application to neutral molecules as models for polypeptides. *J. Phys. Chem.* **1990**, *94*, 4732–4739.
(51) No, K.; Grant, J.; Jhon, M.; Scheraga, H. Determination of net atomic charges using a modified partial equalization of orbital electronegativity method. 2. Application to ionic and aromatic molecules as models for polypeptides. *J. Phys. Chem.* **1990**, *94*, 4740–4746.
(52) Scarsi, M.; Apostolakis, J.; Caflisch, A. Continuum electrostatic energies of macro-molecules in aqueous solutions. *J. Phys. Chem. A* **1997**, *101*, 8098–8106.
(53) Budin, N.; Majeux, N.; Caflisch, A. Fragment-based flexible ligand docking by evolutionary opimization. *Biol. Chem.* **2001**, *382*, 1365–1372.
(54) Cecchini, M.; Kolb, P.; Majeux, N.; Caflisch, A. Automated docking of highly flexible ligands by genetic algorithms: a critical assessment. *J. Comput. Chem.* **2004**, *25*, 412–422.
(55) Huang, D.; Luthi, U.; Kolb, P.; Cecchini, M.; Barberis, A.; Caflisch, A. In silico discovery of β-secretase inhibitors. *J. Am. Chem. Soc.* **2006**, *128*, 5436–5443.
(56) Bodenreider, C.; et al. Identification of lead-like and non-lead-like inhibitors for the dengue virus NS2B/NS3 protease by tryptophan fluorescence. Submitted.
(57) Zhang, Y. L.; Zhang, Z. Y. Low-affinity binding determined by titration calorimetry using a high-affinity coupling ligand: a thermodynamic study of ligand binding to protein tyrosine phosphatase 1b. *Anal. Biochem.* **1998**, *261*, 139–148.
(58) Su, X.-C.; Ozawa, K.; Yagi, H.; Lim, S. P.; Wen, D.; Ekonomiuk, D.; Huang, D.; Keller, T. H.; Sonntag, S.; Caflisch, A.; Vasudevan, S. G.; Otting, G. Low-molecular weight inhibitors stabilize the active conformation of the West Nile virus NS2B-NS3 protease: an NMR analysis. *FEBS J.*, doi:10.1111/j.1742-4658.2009.07132.x.
(59) Shiryaev, S. A.; Aleshin, A. E.; Ratnikov, B. I.; Smith, J. W.; Liddington, R. C.; Strongin, A. Y. Expression and purification of a two-component flaviviral proteinase resistant to autocleavage at the NS2B-NS3 junction region. *Protein Exprression Purif.* **2007**, *52*, 334–339.
(60) Sanchez-Pedregal, V. M.; Reese, M.; Meiler, J.; Blommers, M. J. J.; Griesinger, C.; Carlomagno, T. The INPHARMA method: protein-mediated interligand NOEs for pharmacophore mapping. *Angew. Chem., Int. Ed.* **2005**, *44*, 4172–4175.
(61) Aronov, A. M.; McClain, B.; Moody, C. S.; Murcko, M. A. Kinase-likeness and kinase-privileged fragments: toward virtual polypharmacology. *J. Med. Chem.* **2008**, *51*, 1214–1222.
(62) Fejzo, J.; Lepre, C. A.; Peng, J. W.; Bemis, G. W.; Murcko, M. A.; Moore, J. M. The SHAPES strategy: an NMR-based approach for lead generation in drug discovery. *Chem. Biol.* **1999**, *6*, 755–769.
(63) Kolb, P.; Berset, C.; Huang, D.; Caflisch, A. Structure-based tailoring of compound libraries for high-throughput screening: discovery of novel EphB4 kinase inhibitors. *Proteins: Struct., Funct., Bioinf.* **2008**, *73*, 11–18.
(64) Hopkins, A. L.; Groom, C. R.; Alex, A. Ligand efficiency: a useful metric for lead selection. *Drug Discovery Today* **2004**, *9*, 430–431.
(65) Baker, N. A.; Sept, D.; Joseph, S.; Holst, M. J.; McCammon, J. A. Electrostatics of nanosystems: application to microtubules and the ribosome. *Proc. Natl. Acad. Sci. U.S.A.* **2001**, *98*, 10037–10041.
(66) Wallace, A. C.; Laskowski, R. A.; Thornton, J. M. LIGPLOT: a program to generate schematic diagrams of protein-ligand interactions. *Protein Eng.* **1995**, *8*, 127–134.